Article

AgNWs–Silane Coatings for the Functionalization of Aramid Woven Fabrics

Alicja Nejman [1,*], Anna Baranowska-Korczyc [1], Grzegorz Celichowski [2] and Małgorzata Cieślak [1]

1   Department of Chemical Textiles Technologies, LUKASIEWICZ Research Network—Lodz Institute of Technology, Maria Sklodowska-Curie St. 19/27, 90-570 Lodz, Poland; anna.baranowska-korczyc@lit.lukasiewicz.gov.pl (A.B.-K.); malgorzata.cieslak@lit.lukasiewicz.gov.pl (M.C.)
2   Department of Materials Technology and Chemistry, Faculty of Chemistry, University of Lodz, Pomorska St. 163, 90-236 Lodz, Poland; grzegorz.celichowski@chemia.uni.lodz.pl
*   Correspondence: alicja.nejman@lit.lukasiewicz.gov.pl; Tel.: +48-42-2534494

Abstract: Aramid woven fabrics are widely used to provide protection in extreme conditions, especially in high temperatures. Multifunctional aramid fabrics with no deteriorated thermal resistance and antibacterial properties are needed for high-risk professions. In this study, silver nanowires (AgNWs) and silanes (S) were used for the functionalization of meta- (mAr) and para-aramid (pAr) woven fabrics by mixture (Ag + S) or by the layer-by-layer (Ag/S) method. Antibacterial properties, thermal management, and stability were studied to select the functionalization method which provided the highest thermal performance, comfort, and bioactivity. Both methods decreased the fabric's surface temperature during heating in the range of 35–40 °C by 3 °C and 2 °C, respectively, for mAr and pAr, in comparison to unmodified fabrics. After Ag + S and Ag/S modifications, the thermal degradation initial temperature increased from 554 °C to 560 °C (TG/DTG) and from 525 °C to 533 °C (DSC) for pAr fabrics, and decreased from 417 °C to 403 °C (TG/DTG) and from 411 °C to 406 °C (DSC) for mAr fabrics. The reduction in Gram− (*Klebsiella pneumonia*) and Gram+ (*Staphylococcus aureus*) bacterial growth for all modified samples was above 90%. The bactericidal and bacteriostatic coefficients were slightly higher for Ag/S functionalization. The highest thermal performance and antimicrobial activity were noted for pAr fabric modified using the Ag/S method.

Keywords: meta- and para-aramid woven fabric; silver nanowires; active infrared thermography; differential scanning calorimetry; thermogravimetric analysis; antibacterial properties

1. Introduction

Aramids are aromatic polyamides, characterized mainly by high thermal stability and excellent mechanical properties. They are used in many products, e.g., ropes, sound speaker membranes, sails, aircraft parts, tires, bulletproof vests, etc. A significant area of application for aramid textile materials is special clothing for high-risk professions, e.g., firefighters. Working in dangerous conditions, such as around fire, with contact with objects of very high temperature, or near thermal and UV radiation, requires the use of specific protective materials. An important requirement for such clothing is to ensure thermal comfort by slowing down or preventing an increase in human body temperature [1–3]. This effect can be achieved by incorporating phase change material (PCM) microcapsules into the structure of the textile material [4], or by applying metallic particles, e.g., silver [5]. The use of silver in the form of nanostructures, especially silver nanowires (AgNWs), for the functionalization of textile materials provides them with many added values, including antibacterial [6–8], electrical [6,9–11], optical [12,13], and UV-resistant [11,14] properties, as well as reflecting the infrared radiation [15,16]. Such multifunctional textile materials can be used in wearable electronic devices, heat transfer management systems, electrostatic discharge protection, etc. Despite the many advantages of aramid textiles, their weakness is low resistance to UV radiation [11]. Modification with AgNWs improves resistance

against UV radiation, but nanowires are exposed to photodegradation, as evidenced by the precipitation of silver particles on the surfaces of the nanowires [11,15]. A combination of silver nanowires with silanes protects AgNWs against photodegradation [11]. Moreover, silanes can extend the functionality of aramid textile materials [11].

The aim of this study was assess the influence of modification with AgNWs and silanes on the thermal management, thermal stability, and antibacterial properties of meta- and para-aramid woven fabrics.

Research on aramid textile materials in this respect is a novelty and has not been conducted so far. The obtained results have a significant impact on the development of knowledge in the field of textile materials, nanotechnology, and coating methods. Thanks to the combination of the AgNWs' and silanes' properties, we developed multifunctional aramid textile materials. We also studied the impact of the coating application methods on the modification effect of two types of aramids. Such aramid textiles with special properties can be used in many fields to improve occupational safety and extending the service life of special clothing, e.g., in the automotive and military industry, in protective clothing for high-risk occupations, and in biomedical applications, as well as in daily life as a textile material for curtains, roller blinds, etc.

2. Materials and Methods

2.1. Materials

Meta-aramid (poly (isophthalates-1,3-fenylodiamid)) (mAr) (Newstar®, Yantai Tayho Advanced Materials Co., Ltd., Yantai, China) and para-aramid (poly (1,4-terephthalate-fenylodiamid)) (pAr) (Kevlar®, DuPont, London, UK) woven fabrics were studied. Both fabrics were designed and made at the Lukasiewicz Research Network—Lodz Institute of Technology using a harness loom (CCI Tech. Inc., New Taipei, Taiwan). Table 1 presents the characteristics of the woven fabrics, and Figure 1 shows the SEM images of the meta- and para-aramid woven fabric surfaces (Figure 1a), as well as a cross-section of the woven fabrics (Figure 1b) and fibers (Figure 1c).

Aramid woven fabrics were modified with AgNWs colloid and silanes. Table 2 shows the studied unmodified and modified aramid woven fabrics and their mass values per unit area. Fabrics were also studied after AgNWs colloid application and before silane layer application, and they were called mAr/Ag for meta- and pAr/Ag for para-aramid fabric. Fabrics modified with the mixture (Ag + S) were called mAr/Ag + S for meta- and pAr/Ag + S for para-aramid woven fabric. Those modified with AgNWs and a layer of silanes (Ag/S) were called mAr/Ag/S and pAr/Ag/S, respectively.

Table 1. Characteristic of aramid woven fabrics.

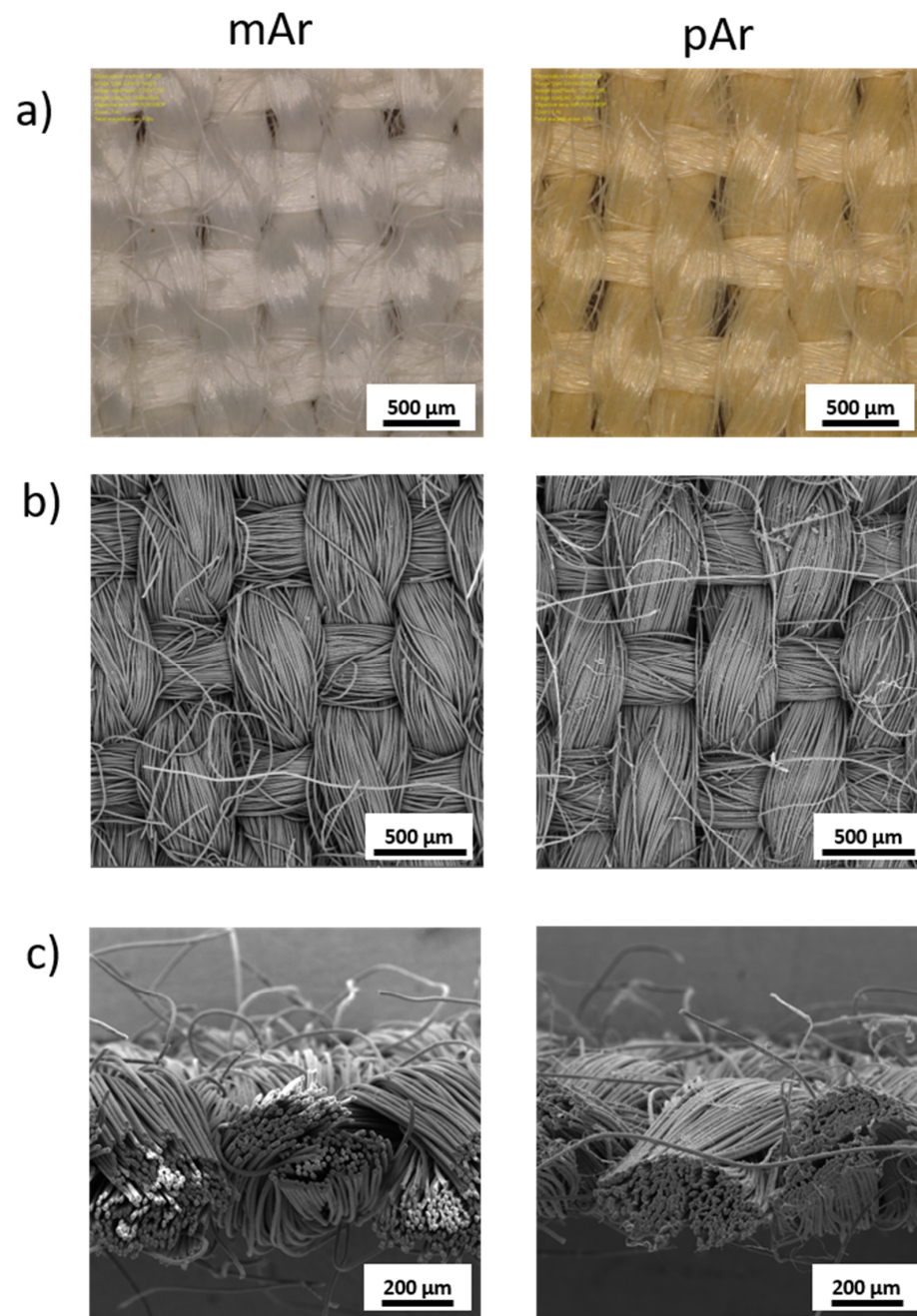| Woven Fabric Parameter		mAr	pAr
Linear mass of yarn, tex		25×2	20×2
Weave		Plain	Plain
Thread number/10 cm	Warp	230	240
	Weft	160	150
Mass per unit area, g/m^2		205 ± 2	165 ± 3
Thickness, mm		0.56 ± 0.01	0.42 ± 0.01
Air permeability, mm/s		299 ± 18	610 ± 18
Volume porosity, %		73.27	72.72

Figure 1. Images of unmodified meta- and para-aramid woven fabrics: (**a**) microscopic and SEM images of fabrics; (**b**) surface; and (**c**) cross section.

Table 2. The list of modified aramid woven fabrics.

	Mass per Unit Area, g/m^2			
Fabric Symbol	**Modified Fabric**	**Ag Coating**	**Silanes (S) Coating**	**Ag/S and Ag + S Coating**
mAr/Ag	248 ± 7	43 ± 2		
mAr/Ag + S	273 ± 7			68 ± 5
mAr/Ag/S	305 ± 9	43 ± 2	62 ± 1	105 ± 3
pAr/Ag	200 ± 1	35 ± 3		
pAr/Ag + S	222 ± 5			57 ± 2
pAr/Ag/S	263 ± 4	35 ± 3	63 ± 5	98 ± 6

2.2. Methods

2.2.1. Synthesis of Silver Nanowire (AgNWs) Colloid

The synthesis of silver nanowires was described in our previous work [6]. In brief, 600 mL of ethylene glycol ($C_2H_6O_2$, Avantor, Gliwice, Poland), 30 g of polyvinylpyrrolidone (PVP, 55,000 g/mol, Sigma Aldrich, Gillingham, UK), and 0.42 g of sodium chloride (NaCl, CHEMPUR, Piekary Śląskie, Poland) were heated to 167 °C and stirred at 150 RPM to obtain a homogenous solution. Next, a mixture of 6.12 g of silver nitrate ($AgNO_3$, 99.9%, Sigma Aldrich, UK) in 300 mL of ethylene glycol was added into the heated solution of ethylene glycol, PVP, and sodium chloride with a peristaltic pump at a rate of 3.33 mL/min for 90 min. After the addition of the silver precursor solution, the colloid was stirred at 150 RPM and heated for 60 min at 167 °C.

After the synthesis, the solution was air-cooled to about 25 °C. To remove ethylene glycol and the excess PVP from the colloid, the solution was diluted with acetone (C_3H_6O, 99.5%, Avantor, Poland) at a ratio of 1:10 and shaken for 10 min. Then, the silver nanowires were dispersed in ethyl alcohol (C_2H_6O, 99.8%, Avantor, Poland).

The concentration of AgNWs in the colloid was 4000 ppm, and the length and diameter of the AgNWs were 10 ± 2 μm and 42 ± 3 nm, respectively [15].

2.2.2. Silane Sol Preparation

The silane sol preparation was described in our previous work [11]. In brief, a mixture of 15.00 g of 3-aminopropyltriethoxysilane (APTES, Unisil, Tarnow, Poland), 1.12 g of diethoxydimethylsilane (DEDMS, Sigma Aldrich, Gillingham, UK), and 3.93 g of 1 M hydrochloric acid (HCl, Avantor, Gliwice, Poland) was shaken for 30 min. Then, ethyl alcohol (C_2H_6O, 99.8%, Avantor, Gliwice, Poland) was added to the solution at 50% by volume of the silane mixture.

2.2.3. Low-Pressure Air RF Plasma Treatment and Polydopamine Modification of Aramid Woven Fabrics

The functionalization of aramid fibers is demanding because of the smooth and chemically inert fiber surfaces; thus, before functionalization, the mAr and pAr woven fabrics were treated with a low-pressure air RF (radio frequency) plasma (Zepto plasma system, Model 2. Diener Electronic, Ebhausen, Germany) for 10 min (Figure 2). The plasma parameters were as follows: pressure, 0.3 mbar; power, 50 W; and generator frequency, 40 kHz. The working gas was air (Linde Gaz, Lodz, Poland), with a composition of 20% O_2 and 80% N_2 (relative humidity (RH) was 40%).

After plasma treatment, to increase the adhesion of silver nanowires to the fiber surfaces, woven fabrics were immersed for 24 h in dopamine solution (2 g/L), which was prepared by dissolving dopamine hydrochloride (Sigma Aldrich, Gillingham, UK) in distilled water and adding tris/glycine buffer (BIO RAD, Warsaw, Poland) to obtain a pH of 8.3. Next, woven fabrics were rinsed with distilled water three times and dried for 24 h at 25 °C.
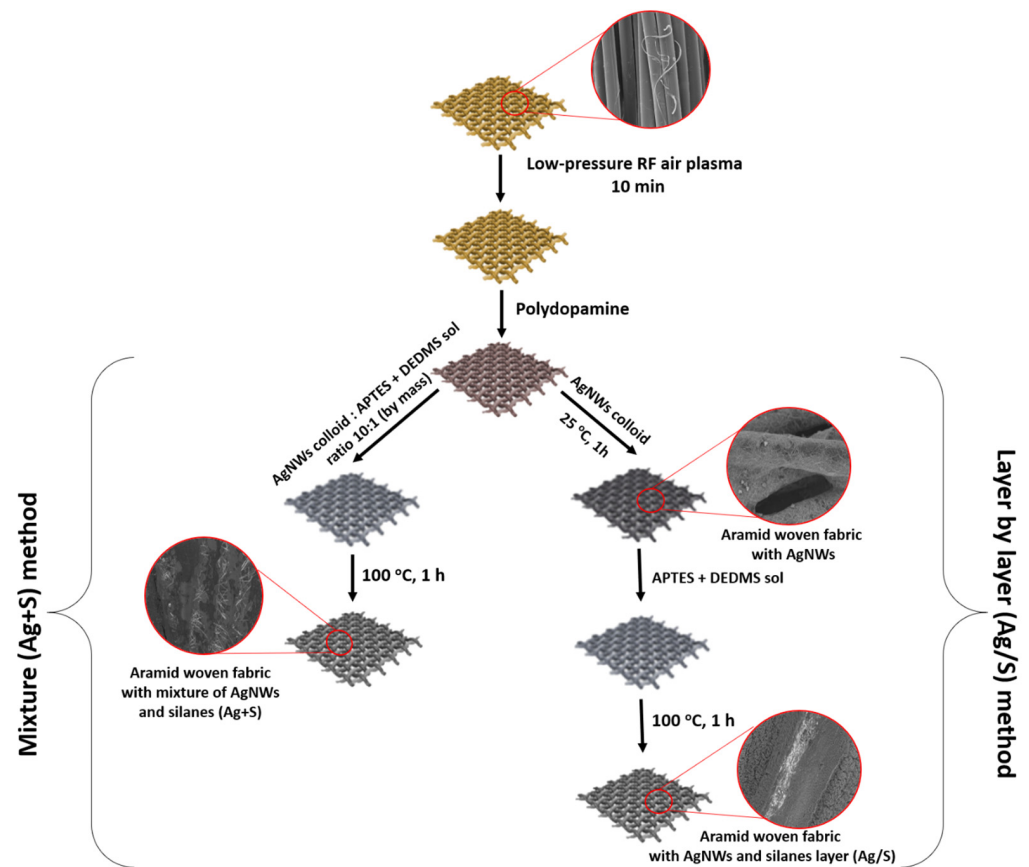
Figure 2. Scheme of aramid woven fabric functionalization.

2.2.4. Functionalization of Aramid Woven Fabrics with AgNWs and Silanes

The functionalization of aramid fabrics with AgNWs and silanes was performed using the one-step (mixture Ag + S) and two-step (layer-by-layer Ag/S) methods (Figure 2), which were described in our previous work [13]. In brief, for the mixture method, the aramid woven fabrics were immersed into the mixture of AgNWs colloid (Ag) and silane sols (S) at a ratio of 10:1 (by mass) for 1 min, then dried in an oven at 100 °C for 1 h. This procedure was repeated 5 times.

For the layer-by-layer method, aramid woven fabrics were immersed in the AgNWs colloid for 1 min and dried at 25 °C. This procedure was repeated 5 times. Next, woven fabrics were dipped 1 time into the silane sols (S), then dried in an oven at 100 °C for 1 h.

2.2.5. Instrumental Techniques

The values of mass per unit area were determined according to the PN-P-04613: 1997 [17]. To determine the values of mass per unit area, five samples with sizes of 10 cm × 10 cm were weighted, and then the values of obtained mass were calculated per 1 m^2 and averaged.

The thickness was measured according to the PN-EN ISO 5089: 1999 [18], using a GM-70 unit (Lukasiewicz-Lodz Institute of Technology, Lodz, Poland) with a pressure-foot of 200 Pa. Ten samples with diameters of 5 cm were measured, and the average value of the thickness was calculated.

The air permeability was assessed according to the PN-EN ISO 9237 [19], using a TEXTEST unit type SX-3300 (Textest AG, Schwerzenbach, Switzerland). Ten samples with diameters of 5 cm were measured, and the average value of the air permeability of the woven fabrics was calculated.

Microscopic imaging was performed on a digital optical microscope, DSX 1000 (OLYM-PUS, Tokyo, Japan), with a magnification of 300×.

SEM analysis was carried out using a VEGA 3 scanning electron microscope (TESCAN, Brno, Czech Republic) and a Nova NanoSEM 450 scanning and transmission microscope (FEI, Hillsboro, OR, USA). The samples were placed onto a microscope platform (diameter 12 mm) using an adhesive carbon disc. The fibers for cross-sectional images were cut with a scalpel and placed on a specially prepared holder in an upright position. Microscopic images of the fiber surface were taken at magnifications of $100\times$, $200\times$, $1000\times$, and $2500\times$.

The content of silver was tested using an Agilent 240FS Atomic Absorption Spectrometer (Agilent Technologies, Santa Clara, CA, USA). The modified woven fabrics, with weights of 2–6 mg, were ground and placed into a Kiejdahl flask, and 5 mL of concentrated nitric acid (HNO_3, CHEMPUR, Piekary Śląskie, Poland) was added. The sample was heated in a mineralizer in a fume cupboard until it was completely dissolved. The obtained clear solution was quantitatively transferred to a volumetric flask and then filled up to 50 mL with demineralized water. The absorbance was measured at a wavelength of 328 nm. Three samples of each modified woven fabric were analyzed.

FTIR-ATR spectra were performed using a Vertex 70 FTIR spectrometer (Bruker, Mannheim, Germany) at a resolution of 4 cm^{-1}, in the range of 600–4400 cm^{-1}.

Raman spectra were recorded using a Renishaw InVia Reflex Raman spectrometer with a Leica microscope (Renishaw, Gloucestershire, UK), and a near-infrared semiconductor laser (λ = 785 nm) was used as the excitation source. The laser beam was focused on the samples with a $50\times$ objective lens.

Investigations of thermal properties were carried out using the differential scanning calorimeter DSC 204 F1 Phoenix (Netzsch, Selb, Germany). AgNWs, PVP, and woven fabric samples with weighing about 5 mg were placed into a ceramic crucible with a volume of 85 μL, then heated in the temperature range of 20–600 °C with a rate of 10 °C/min under nitrogen (gas flow of 20 mL/min). Three samples of AgNWs, PVP, and woven fabrics were analyzed. The initial (T_{Onset}), final (T_{End}), and peak maxima (T_{Peak}) temperatures, as well as the heat during thermal decomposition (ΔH_{Deg}), were determined.

Thermogravimetric analysis (TG/DTG) was carried out using a TG 209 F1 Libra (Netzsch, Selb, Germany) thermogravimetric analyzer. Samples of AgNWs, PVP, and woven fabrics weighing about 5 mg were tested in a ceramic crucible with a volume of 85 μL in a nitrogen atmosphere (gas flow of 25 mL/min), then heated in the temperature range of 30–800 °C at a heating rate of 10 °C/min. Three samples of AgNWs, PVP, and woven fabrics were measured. The initial (T_{Onset}), final (T_{End}), and peak maxima (T_{Peak}) temperature of the thermal degradation process, as well as the weight losses of the samples, were determined.

The active infrared thermography analysis was performed using the VarioCAM thermal imaging camera (InfraTec., Dresden, Germany), recording thermograms in the form of images with resolutions of 640 × 480 pixels. The camera was equipped with an uncooled, microbolometric detector with a spectral range of 8–13 mm. The samples were placed onto a hotplate with a specified temperature in the range of 35–40 °C. The distance of the camera from the hotplate's surface was 1 m. Measurements were made at a temperature of 23.4 ± 0.1 °C, and the relative humidity (RH) was 75 ± 2%. For each specified temperature, 20 thermograms were made and recorded every 1 s. The processing and analysis of the obtained thermograms was performed in the IRBIS V2.2 program.

The antibacterial properties were assessed according to the standard test method AATCC 100-2012 [20]. The quantitative assessment was made on the basis of the PN-EN ISO 20743 [21]. In the research, *Staphylococcus aureus* (ATCC 6538, Gram-positive) and *Klebsiella pneumoniae* (ATCC 4352, Gram-negative) bacteria were used. *S. aureus* bacteria, at a concentration of 1.8×10^5 CFU/mil, and *K. pneumoniae*, at a concentration of 1.5×10^5 CFU/mil, were applied to the woven fabrics. The incubation time was 21 h + 48 h at 37 ± 2 °C.

3. Results and Discussion

3.1. Application Effect of Coatings

The value of mass per unit area of Ag + S coating was lower for the para-aramid woven fabric than for the meta-aramid. This was due to differences in the structures (Figure 1) and parameters (Table 1) of both aramid woven fabrics. The air permeability of the unmodified mAr woven fabric was two times lower than that of the pAr woven fabric, and the linear weight of the meta-aramid yarn was also higher (Table 1). This caused the greater thickness and available surface of meta-aramid woven fabric. As a result, more silver nanowires and silanes were deposited both on the surfaces of the fibers and in the spaces between them compared to the para-aramid woven fabric.

In the case of the Ag/S method, one layer of silanes was applied onto the earlier deposited uniform AgNWs coating, which is why the masses per unit area of the silane layer are comparable for both types of aramid fabrics.

3.2. SEM Analysis

In the case of application of AgNWs (Ag), the SEM images show aramid fibers covered by the AgNWs network (Figure 3). For all modified fabrics, AgNWs were found on the surfaces of the fibers and inside the fabric structure. After mixture modification (Ag + S) (Figure 3a,b), silver nanowires were embedded in the silanes. For the layer-by-layer (Ag/S) method (Figure 3a,b), the silane layer covered the surfaces of the AgNWs.
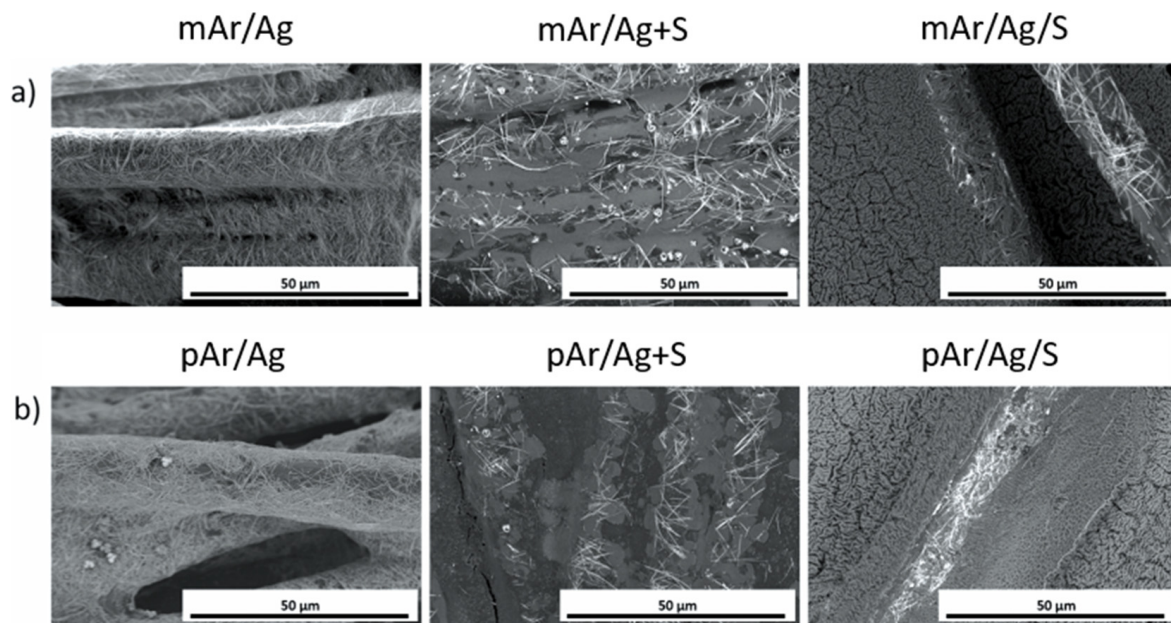

Figure 3. SEM images of (**a**) meta- and (**b**) para-aramid woven fabrics after AgNWs (Ag) application and the use of the mixture (Ag + S) and layer-by-layer (Ag/S) methods.

3.3. AAS Analysis

The AAS analysis demonstrated that the Ag content in the fabrics with only AgNWs coatings amounted to 32 g/kg for the mAr/Ag (Figure 4a) and 25 g/kg for the pAr/Ag fabric (Figure 4b). The higher silver content in the meta- than in the para-aramid fabric was due to the greater surface available for AgNWs application on meta-aramid fabric (Figure 1). The silver content for fabrics with Ag/S coatings amounted to 17 g/kg, and for those with Ag + S coatings, 15 g/kg. This differences between fabrics coated with only AgNWs and those with silanes resulted from the calculation of the mass of the whole sample. The presence of silanes reduced the ratio of the silver content to the other components of the sample in the modified fabric.
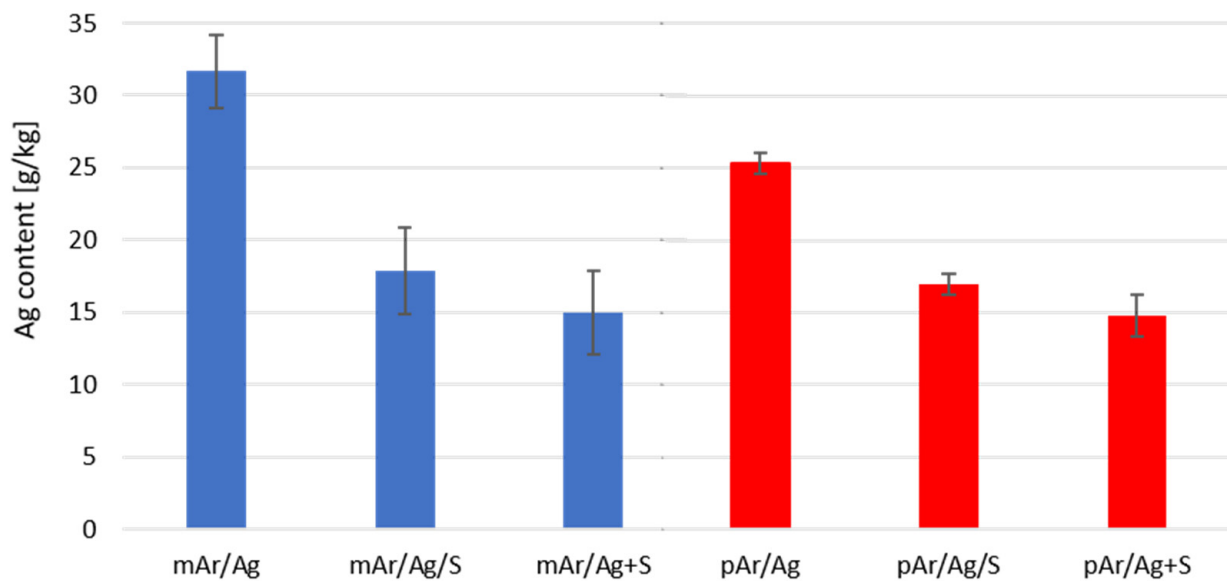
Figure 4. Silver content from AAS analysis for modified meta- and para-aramid woven fabrics.

3.4. FTIR Analysis

In order to verify the influence of the coatings on both aramid fabrics, they were analyzed using infrared spectroscopy.

In the FTIR spectrum of unmodified mAr fabric (Figure 5a), the band at 3291 cm^{-1} indicates the presence of stretching vibrations of the N-H group. The band at 1647 cm^{-1} corresponds to the stretching vibrations of the C=O and C-N groups. At 1602 cm^{-1}, the C=C stretching vibrations of the aromatic ring can be observed. The peak at 1525 cm^{-1} indicates the presence of N-H in plane bending vibrations and C-N stretching coupled modes of the C-N-H group. The band at 1299 cm^{-1} designates aromatic C-N stretching vibrations. The band at 1239 cm^{-1} corresponds to the stretching vibrations of the C-N group, the N-H in-plane bending vibrations, and the stretching vibrations of the C-C bond (Amide III). The peak of C-H out-of-plane bond in the meta-substituted aromatic ring appears at 779 cm^{-1}. At 715 cm^{-1}, the band of N-H out-of-plane bending vibrations can be observed. The band at 682 cm^{-1} indicates the presence of an out-of-plane C-H bond in the meta-substituted aromatic ring.

For the unmodified pAr fabric (Figure 5b), the band at 3314 cm^{-1} corresponds to the stretching vibrations of the N-H group. The band at 1647 cm^{-1} indicates the stretching vibrations of the C=O group. At 1536 cm^{-1}, the band of stretching vibrations of the N-H group can be observed. The bands at 1510 cm^{-1} and 1304 cm^{-1} indicate the stretching vibrations of the C=C and C-N groups, respectively. The p-substituted phenyl band can be observed at 863 cm^{-1}.

In the FTIR spectrum of silanes, the characteristic bands of -Si-O-Si- and -Si-O-C- bonds are present at 1000 cm^{-1} and 1100 cm^{-1} [22,23]. These bands can also be observed in the FTIR spectra for AgNWs- and silane-modified meta-aramid fabrics (Figure 5a,b), at 1034 cm^{-1} and 1102 cm^{-1} for mixture and at 1003 cm^{-1} and 1088 cm^{-1} for layer-by-layer modified fabrics. For para-aramid fabrics, these bands occurred at 1008 cm^{-1} and 1102 cm^{-1} for the mixture and at 1003 cm^{-1} and 1087 cm^{-1} for the layer-by-layer method.

The presence of silver nanowires could not be identified using FTIR analysis; therefore, the assessment was conducted indirectly by analyzing the presence of the PVP with which the silver nanowires were covered.
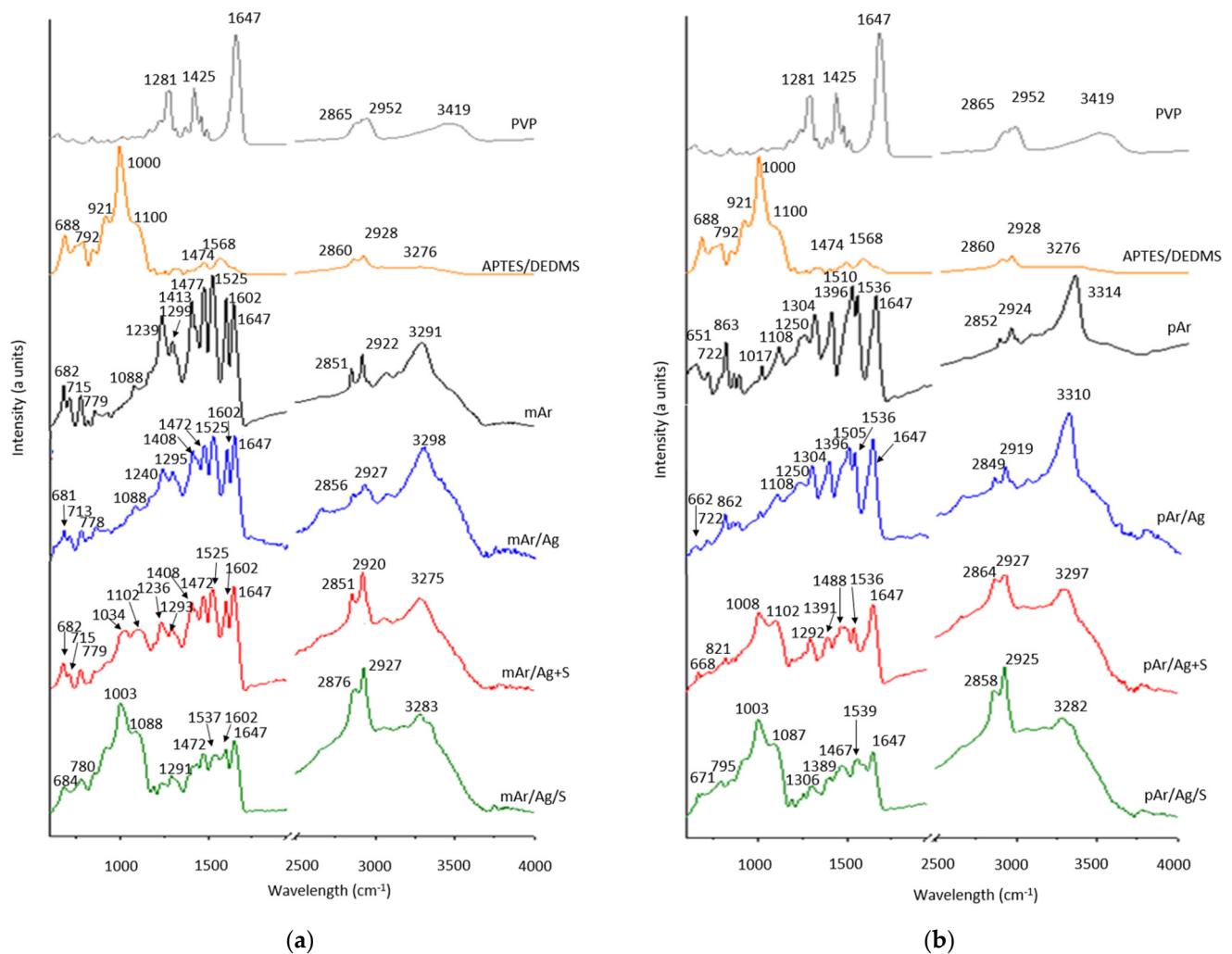
Figure 5. FTIR spectra of PVP, mixture of silanes and unmodified and modified (**a**) meta- and (**b**) para-aramid woven fabrics.

In the FTIR spectrum of PVP powder (Figure 5), the band at 3419 cm^{-1} and the double band, with maxima at 2952 cm^{-1} and 2865 cm^{-1}, correspond to O-H and C-H stretching vibrations, respectively. The intense characteristic band at 1647 cm^{-1} corresponds to the stretching vibrations of the C=O group. The bands at 1281 cm^{-1} and 1425 cm^{-1} refer to the C–N stretching vibrations and -CH$_2$ groups in the PVP pyrrole ring.

For all modified fabrics, an increase in the intensity of the characteristic band of C=O at 1647 cm^{-1} was observed. The same band was observed in the spectra of unmodified fabrics and PVP. This intensity increase may indicate that the fibers were covered with silver nanowires and PVP. Due to the overlapping, both bands originated from unmodified fabrics and PVP. The complementary technique of Raman spectroscopy was applied to this study.

3.5. Raman Analysis

Raman spectroscopy allows us to study coating presence and molecule conformation on textile structures. It was implemented in the study as a complementary technique to infrared analysis. In order to assess the effectiveness of AgNWs and silane application, Raman spectroscopic analysis was performed (Figure 6) for unmodified meta-and para-aramid fabrics, PVP, AgNWs colloid, silanes, and fabrics modified with AgNWs and silanes.
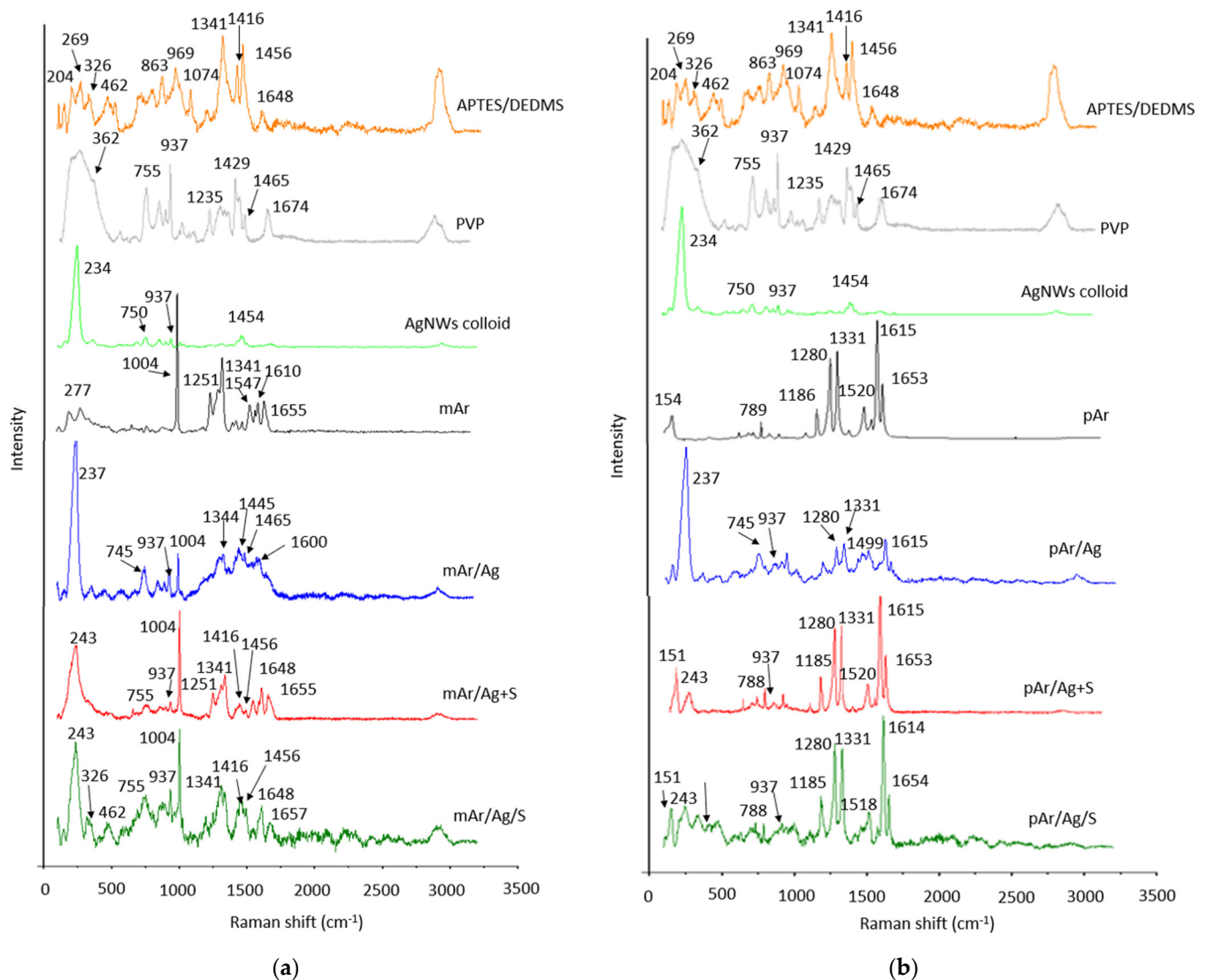
Figure 6. Raman spectra of PVP, mixture of silanes, AgNWs colloid, unmodified and modified (**a**) meta- and (**b**) para-aramid woven fabrics.

In the Raman spectrum for the unmodified mAr fabric (Figure 6a), the band at 1655 cm^{-1} indicates the presence of stretching vibrations of the C=O group (Amide I). At 1610 cm^{-1}, the band of C-C bond vibrations in the aromatic ring can be seen. The bands at 1547 cm^{-1} correspond to the in-plane bending vibrations of the N-H group, while the band at 1341 cm^{-1} indicates bending vibrations in-plane of the aromatic ring of the C-H group. At 1251 cm^{-1}, the bands of bending vibrations of the N-H group and stretching vibrations of the C-N group are observed. The band at 1004 cm^{-1} is characteristic of deformation vibrations of the C-H group in the aromatic ring.

For unmodified pAr fabric (Figure 6b), the band at 1653 cm^{-1} indicates stretching vibrations of C=O group (Amide I). The band at 1615 cm^{-1} corresponds to the stretching vibrations of the C-C bond in the aromatic ring. The bands at 1520 cm^{-1} and 1331 cm^{-1} indicate the bending vibrations of the C-H group in the aromatic ring. The peak at 1280 cm^{-1} corresponds to the bending vibrations of the N-H group and the stretching vibrations of the C-N group. At 1186 cm^{-1}, the band of deformation vibrations of the C-H group in the aromatic ring occurred. The band at 789 cm^{-1} indicates the presence of out-of-plane deformation vibrations of the C-H group and deformation vibrations of the C-C-C bond in the aromatic ring.

PVP powder was studied due to its presence on the AgNWs surface, because this polymer acts as a capping agent during nanowire synthesis and is also evidence of AgNWs' presence in the coating. In the Raman spectrum for PVP powder (Figure 6), there are bands at 755 cm^{-1} corresponding to the stretching vibrations of the C–N group; at 937 cm^{-1} corresponding to the stretching vibrations of the C–C group; and at 1235 and 1429 cm^{-1} indicating the stretching vibration of the C–N group and the bending vibrations of the C–H group, respectively.

The spectrum of the AgNWs colloid contains characteristic bands originating from PVP at 750 cm^{-1} and 937 cm^{-1}. There is also a band at 234 cm^{-1}, which is characteristic of Ag-O stretching/bending vibrations, indicating the interaction between silver and oxygen molecules adsorbed on its surface [24].

In the Raman spectrum of fabrics modified with silver nanowires, the additional bands characteristic of PVP and AgNWs are present. These include one centered at 237 cm^{-1}, indicating the presence of Ag-O vibration, and typical PVP bands at 745 cm^{-1} and 936 cm^{-1}. The intensity of the other aramid bands decreased, especially the meta-aramid band of the C-H bond in the aromatic ring at 1004 cm^{-1} (Figure 6a), and bonds in the range of 1200 to 1700 cm^{-1} for para-aramid samples (Figure 6b). This proves that the fabric's surface was effectively coated with silver nanowire colloids.

In this study, part of the coatings of the aramid fabrics consisted of silanes (APTES/ DEDMS). The silane spectrum shows characteristic bands of -Si-O-Si- bonds at 462 cm^{-1} and 1074 cm^{-1} [23,25]. The bands at 1648 cm^{-1} and 1341 cm^{-1} correspond to the amino groups -NH$_2$ and -NH, respectively, and at 1456 cm^{-1} and 1416 cm^{-1}, they indicate the presence of -CH$_2$ and -CN bonds. The band at 969 cm^{-1} indicates the presence of -CH$_2$ and -NH$_2$ groups originating from APTES.

The Raman spectrum of meta-aramid fabrics modified with AgNWs and silanes (Figure 6a) shows a strong band at 243 cm^{-1}, indicating the presence of silver, and bands at 755 cm^{-1} and 937 cm^{-1}, characteristic of PVP. The bands originating from silanes occur at 462 cm^{-1}, which indicates the presence of a -Si-O-Si- bond, and the bands at 1648 cm^{-1} and 1341 cm^{-1} correspond with the amino groups -NH$_2$ and -NH. Those at 1456 cm^{-1} and 1416 cm^{-1} confirm the presence of -CH$_2$ and -CN bonds. In the case of para-aramid fabrics modified with AgNWs and silanes (Figure 6b), a band at 243 cm^{-1} is also visible, confirming the presence of silver. The band at 937 cm^{-1} is characteristic of PVP. The presence of silanes on the fabric surface is confirmed by the band at 462 cm^{-1}, attributed to the -Si-O-Si- bond, and the band at 969 cm^{-1}, attributed to the -CH$_2$ and -NH$_2$ bonds. The spectra for modified fabrics show both components of the applied coating of AgNWs and silanes, and prove the effectiveness of the formation of the coating on the surfaces of the fabrics.

3.6. Active Infrared Thermography

To assess the thermal management ability of unmodified and modified aramid woven fabrics, active infrared thermography was used. The temperature range from 35 to 40 °C was chosen as it is close to human body temperature. It was found that the dependencies between the temperature of the woven fabric surface and the temperature of the hotplate surface, after heating, was linear (Figure 7).

The temperature values of unmodified mAr fabric (33.8–37.1 °C) (Figure 7a) were higher than those of pAr fabric (34.1–37.6 °C) (Figure 7b) by about 0.5 °C. There was a lower value of air permeability for mAr than for pAr fabric (Table 1), and the greater volume of air was found in the mAr fabric structure. The thermal conductivity of the air amounted to 0.025 Wm^{-1}K^{-1}. A higher value of thermal conductivity was found for meta-aramid (0.13 Wm^{-1}K^{-1}) compared to para-aramid (0.04 Wm^{-1}K^{-1}). The higher mass per unit area, thickness, and volume porosity (Table 1) caused the surface of the mAr fabric to have a higher temperature.
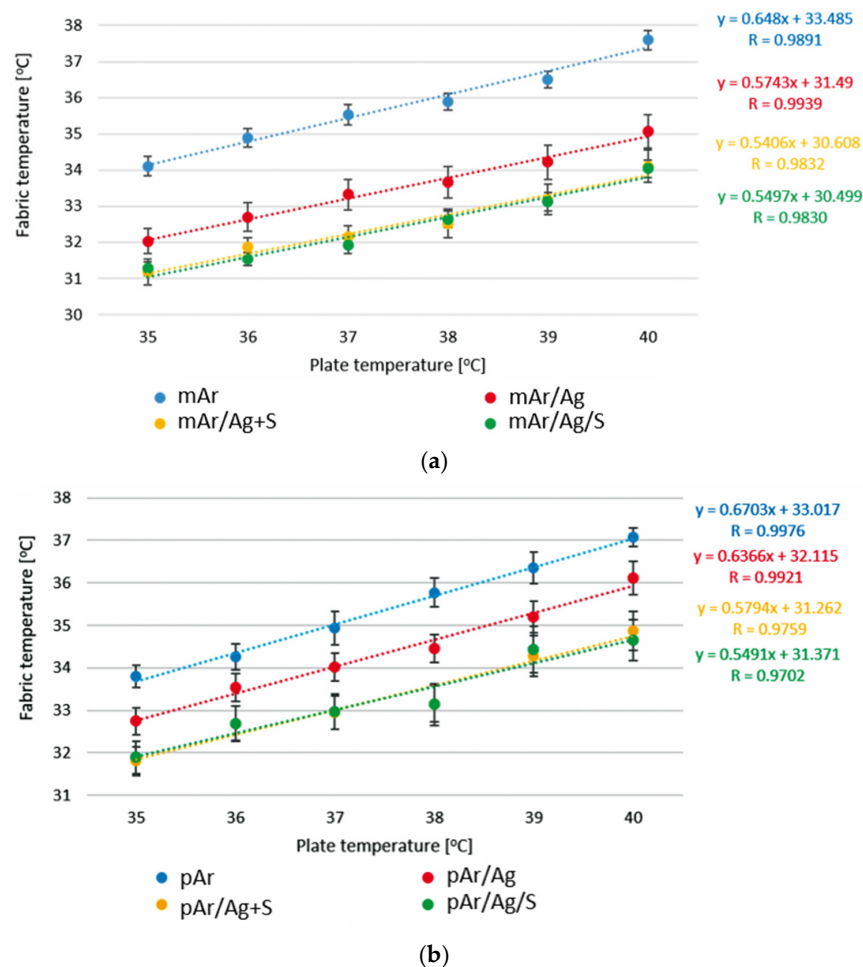
(a)

(b)

Figure 7. Temperature changes in unmodified and modified (**a**) meta- and (**b**) para-aramid woven fabrics after 20 s of heating.

Both aramid fabrics functionalized with AgNWs had lower surface temperatures than unmodified fabrics, by about 2 °C (32.0–35.1 °C) for mAr/Ag and by about 1 °C (32.7–36.1 °C) for pAr/Ag fabric. A similar phenomenon was also observed in our previous work for para-aramid fabric ultrasonic spray-coated with an aqueous solution of AgNWs [15]. AgNWs-modified fabrics showed better thermal radiation insulation properties [26,27] and a better ability to reflect infrared radiation than unmodified fabrics. The mAr/Ag fabric had lower temperatures than the pAr/Ag fabric by about 1 °C. This may be due to the higher silver content in the mAr than in the pAr fabric (Figure 4). The mass per unit area of the AgNWs coating for the mAr fabric was higher (Table 2); this is related to the higher linear mass of meta-aramid yarn. The higher mass per surface area and greater thickness (Table 1), as well as the greater surface area available for modification, allowed for the application of more silver nanowires.

Figure 7 shows that fabrics modified with AgNWs and silanes had the lowest surface temperatures. The presence of silanes decreased the surface temperatures of both fabrics by about 1 °C compared to the fabrics modified with only AgNWs. Air, which is an insulator, filled the spaces in the structure of the fabric, and the applied silanes covered the surface of the aramid fabric, limiting the penetration of infrared radiation. Moreover, AgNWs reflect infrared radiation, which additionally prevents heat transfer. In the entire range of heating temperatures, the differences between the surface temperatures of unmodified fabrics and those modified with AgNWs and silanes, with both methods, amounted about 3 °C for mAr (Figure 7a) and about 2 °C for pAr (Figure 7b) fabric. Lower temperature values for modified than for unmodified fabrics were confirmed by thermal images of the fabric

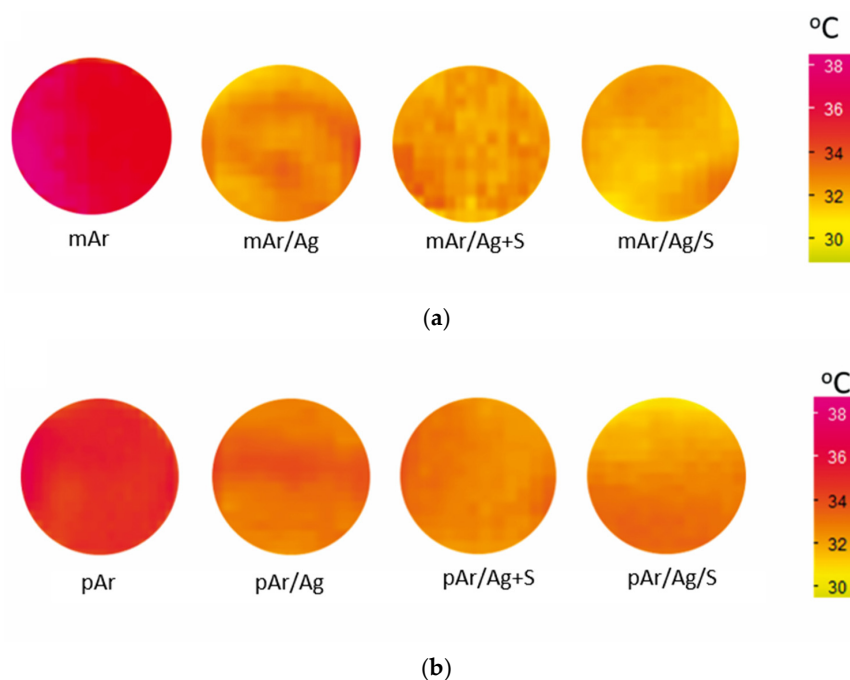surfaces (Figure 8) at the selected temperature of 36 °C, which is marked in orange/yellow.

(**a**)

(**b**)

Figure 8. Examples of images recorded by an infrared camera of unmodified and modified (**a**) meta- and (**b**) para-aramid woven fabrics after 20 s of heating at 36 °C.

3.7. TG/DTG Analysis

The TG/DTG analysis was performed in order to investigate the impact of functionalization on the thermal stability of meta- and para-aramid fabrics.

The thermal degradation of the AgNWs began at a temperature of 390 °C, with a peak maximum temperature of 422 °C. This peak was assigned to the PVP powder, used for the synthesis of AgNWs, and colloid stabilization (Figure 9). The initial temperature of PVP thermal decomposition was 398 °C. Based on the weight loss of pure PVP and AgNWs (98% and 65%, respectively), the calculated AgNWs content amounted to 33%. Usmanova et al. [28] found that thermal degradation of PVP occurred above 390 °C, leading to weight loss of more than 90%.
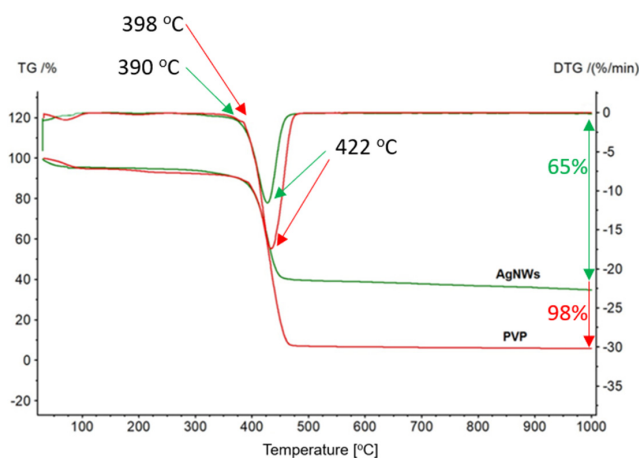

Figure 9. TG/DTG thermograms for PVP and AgNWs.

The TG analysis for both unmodified fabrics showed a slight weight loss in the temperature range of 30–120 °C and corresponding peaks on the DTG curves, indicating the water desorption process (Figure 10, Table S1).
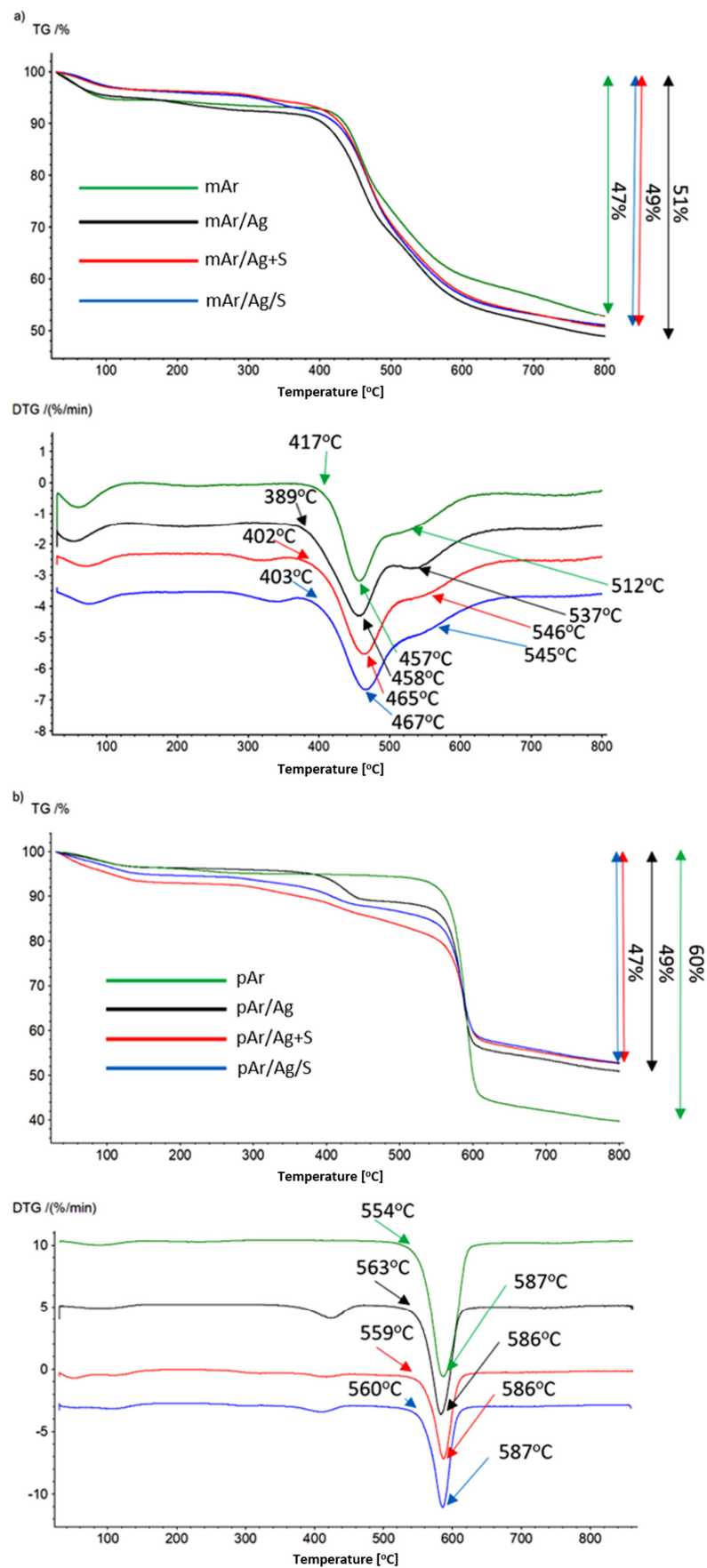
Figure 10. TG/DTG thermograms for (**a**) meta- and (**b**) para-aramid woven fabrics, both unmodified and modified by AgNWs through the mixture (Ag + S) and layer-by-layer (Ag/S) methods.

The thermal decomposition process of unmodified mAr fabric began at 417 °C and took place in two stages, with maximum peaks at 457 °C and 512 °C (Figure 10a, Table S1). The weight loss of the mAr fabric in the temperature range of thermal degradation amounted to 36%. At a temperature of 800 °C, the total weight loss of the fabric was 47%.

The application of AgNWs on meta-aramid fabric caused a decrease in the initial temperature of thermal degradation of 28 °C (Figure 11). The temperature at the first peak maximum did not change, but for the second peak, it increased by 25 °C. The weight loss in the temperature range of the meta-aramid fabric decomposition was higher by 5% compared to the unmodified mAr fabric. The total weight loss at 800 °C for the mAr/Ag fabric was higher by 4%.
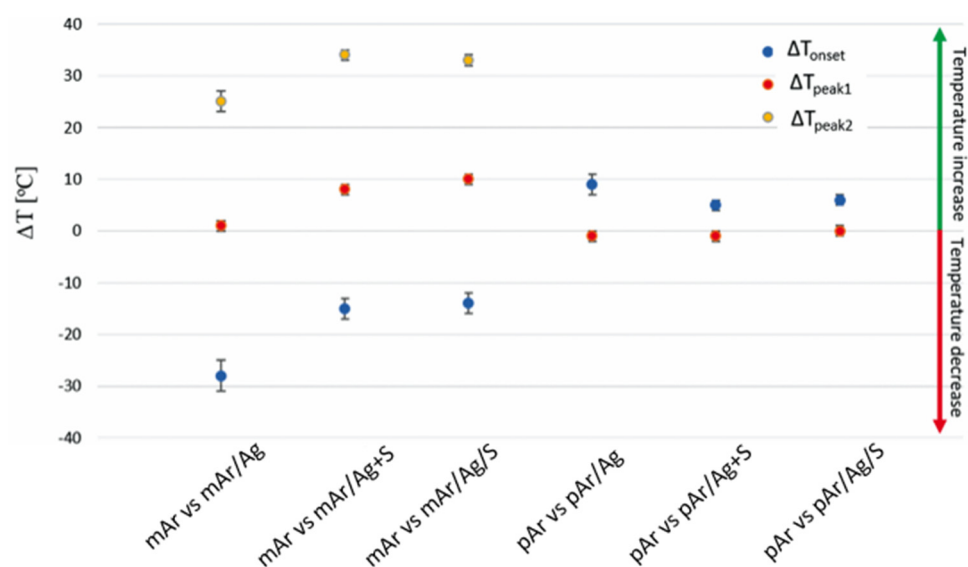

Figure 11. Differences in onset and in first and second decomposition peak maxima between unmodified and modified woven fabrics, according to TG/DTG analysis.

For the mAr/S fabric, in the temperature range of 285–349 °C with a peak maximum at 320 °C, a weight loss of 2% occurred, which was related to the thermal degradation of silanes (Figure 10a, Table S1). For the mAr/Ag/S fabric, silane weight loss of 3% was observed in the range of 297–363 °C, with a peak maximum at 339 °C. For these fabrics, the process of thermal degradation of the meta-aramid fabric was observed above 400 °C. The application of silanes caused increases in the initial temperature of about 13 °C and 14 °C, respectively, for mAr/Ag + S and mAr/Ag/S compared to meta-aramid fabric, with only AgNWs (Figure 11). However, the initial temperatures were lower by 15 °C and 14 °C, respectively, in comparison with the unmodified fabric. The temperatures in the first and second peak maxima were higher by 8 °C and 34 °C for mAr/Ag + S, and by 10 °C and 33 °C for mAr/Ag/S. The weight losses were higher than those of the unmodified mAr fabric, and amounted 40% and 39% for the Ag + S- and the Ag/S-modified fabric, respectively. The total weight loss at 800 °C was 49% for both fabrics.

After modifications, the decrease in the initial temperature of thermal degradation for the meta-aramid fabric was a result of the presence of PVP. The thermal decomposition in the AgNWs colloid began at 390 °C (Table S1). This may have coincided with the process of thermal decomposition of the meta-aramid fabric and shifted its initial temperature towards lower values.

The thermal decomposition process of the unmodified pAr fabric occurred at 554 °C, with a peak maximum at 587 °C (Figure 10b, Table S1). The weight loss in the temperature range of para-aramid fabric thermal degradation amounted to 52%, and the total weight loss at 800 °C was 60%. For the pAr/Ag fabric, heating above 360 °C resulted in weight loss of PVP in the range of 377–449 °C, with the peak maximum at 416 °C. The weight loss of PVP amounted to 6%. Above 550 °C, the thermal degradation of the para-aramid fabric

began. The initial temperature of degradation increased by 9 °C (Figure 11), and did not change at the peak maximum. The weight loss was lower by 16%. The total weight loss at 800 °C for the pAr/Ag fabric was lower by 11% compared to the unmodified pAr fabric. Sun et al. [29] showed that the thermal stability of para-aramid fabric modified with silver nanoparticles did not change. However, the weight loss was lower and amounted to about 40%, while for unmodified fabric, it was about 60%.

In the case of para-aramid fabrics modified with AgNWs and silanes, above 270 °C, the thermal degradation of silanes began at 276 °C, with a peak maximum at 304 °C, for the pAr/Ag + S fabric, and at 286 °C, with a peak maximum at 310 °C, for the pAr/Ag/S fabric (Figure 10b). The silane weight loss amounted to 1% and 2%, respectively, for Ag + S- and Ag/S-modified fabrics. Further heating resulted in weight loss of PVP in the temperature range of 380–443 °C, with a peak maximum at 409 °C, for the pAr/Ag + S fabric, and in the range of 389–452 °C, with a peak maximum at 418 °C, for the pAr/Ag/S fabric. For both of the modified para-aramid fabrics, the heat during the thermal degradation of PVP amounted to 5 J/g. Above 550 °C, the thermal degradation of the para-aramid fabric began. The presence of silanes improved the thermal stability of Ag + S- and Ag/S-coated fabrics in comparison with unmodified fabric. The initial degradation temperatures were higher by 5 °C and 6 °C, respectively, but lower by 4 °C and 3 °C compared to fabrics modified with only AgNWs (Figure 11). The temperature at the peak maximum did not change after the modifications. The weight loss of the para-aramid fabric was lower than for the unmodified fabric by 22% for the pAr/Ag + S and by 24% for pAr/Ag/S fabric. The total weight loss at 800 °C for both modified fabrics was lower than for the unmodified pAr fabric, and amounted to 47%.

3.8. DSC Analysis

The DSC analysis for PVP and AgNWs colloid (Figure 12) showed an endothermic peak in the range of 20–120 °C, indicating the water desorption. The thermal decomposition of the AgNWs colloid was observed at 395 °C, with the peak maximum at 433 °C. This peak was assigned to the thermal degradation of PVP, which stabilized the AgNWs in the colloid, a result that was also found by Giesz et al. [6]. The thermal degradation process of PVP began at 398 °C, with the peak maximum at 433 °C (Figure 12, Table S2). The same temperature values for PVP degradation were obtained by Usmanova et al. [28] and Morsi et al. [30]. The heat of thermal decomposition amounted to 460 J/g for pure PVP and to 417 J/g for the AgNWs colloid.
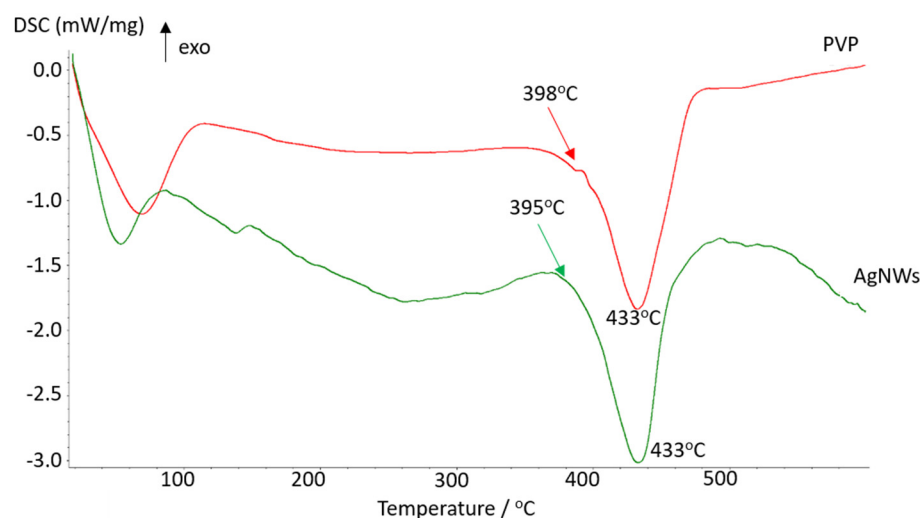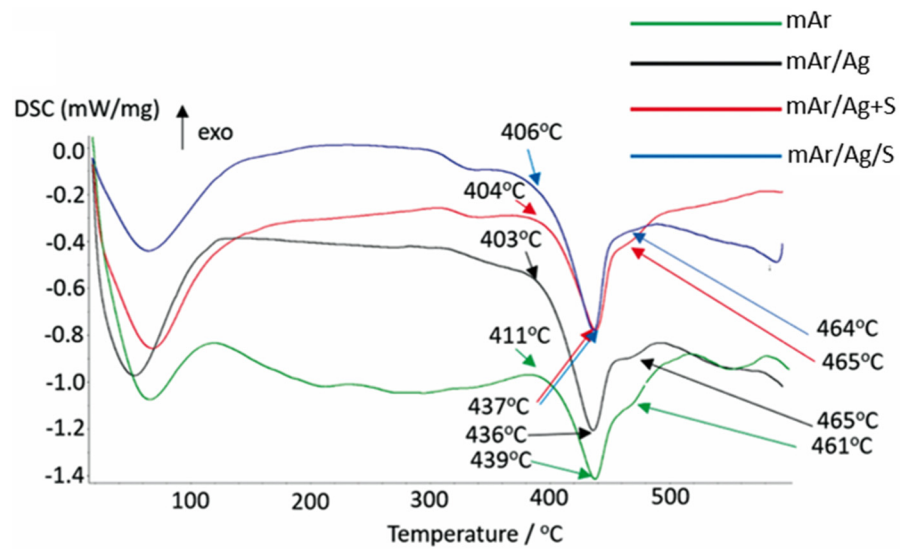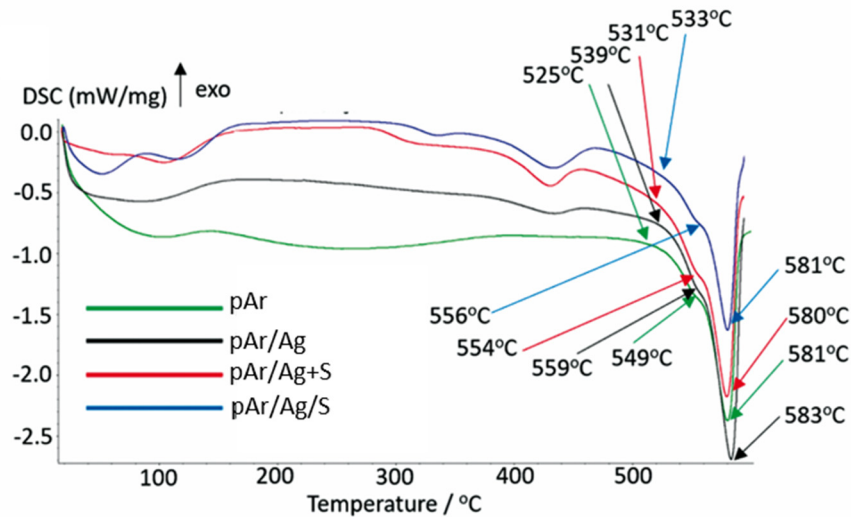

Figure 12. DSC thermograms for PVP and AgNWs colloid.

For both of the unmodified aramid fabrics (Figure 13), the endothermic peak of moisture removal was observed in the range of 20–120 °C.

(a)

(b)

Figure 13. DSC thermograms for (**a**) meta- and (**b**) para-aramid woven fabrics, unmodified and modified with AgNWs, using the mixture (Ag + S) and layer-by-layer (Ag/S) methods.

The degradation process of unmodified mAr fabric began at 411 °C and took place in two stages, with maximum endothermic peaks at 439 °C (first stage) and 461 °C (second stage). The thermal decomposition heat amounted to 100 J/g (Figure 13a, Table S2).

After the application of AgNWs, the initial temperature of degradation decreased by 8 °C (Figure 14). The temperature at the peak maximum of the first stage did not change, and the peak maximum in the second stage was slightly higher, amounting to 465 °C. The heat of thermal degradation increased by 31 J/g.
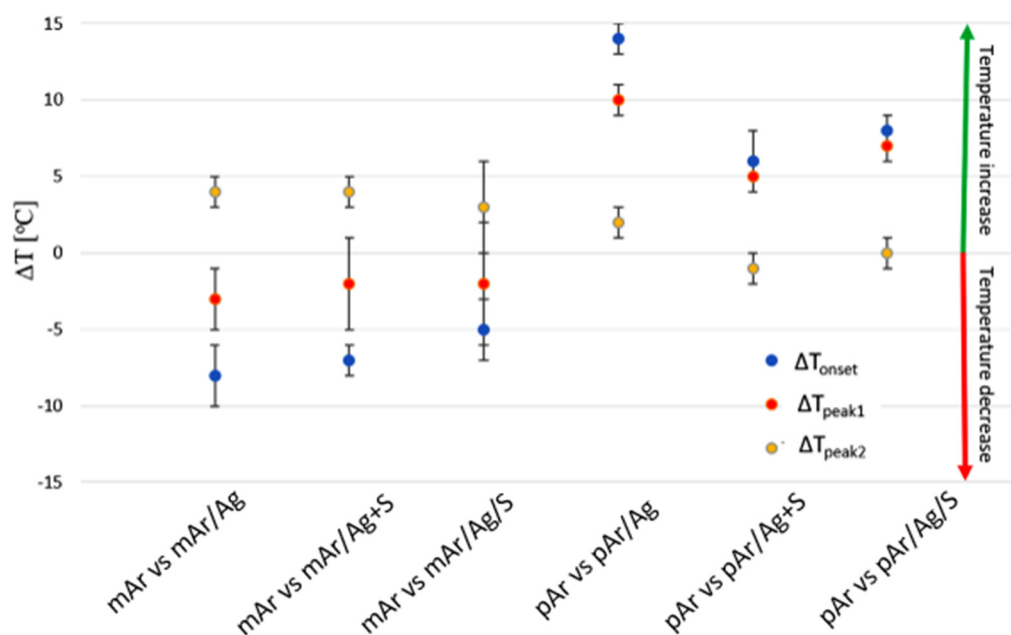
Figure 14. Differences in onset and in first and second decomposition peak maxima between unmodified and modified woven fabrics according to DSC analysis.

For meta-aramid fabrics modified with Ag + S and Ag/S coatings, a peak indicating the presence of silanes was observed. The thermal degradation of the silanes occurred at 316 °C, with a peak maximum at 342 °C, for the mAr/Ag + S fabric, and at 311 °C, with a peak maximum at 331 °C, for the mAr/Ag/S fabric. The heat of the thermal degradation of silanes amounted to 5 J/g for both modified fabrics. Above 400 °C, the thermal degradation of meta-aramid fabric began. The initial temperature was comparable with only AgNWs, but was lower by 7 °C for the mAr/Ag + S fabric and by 5 °C for the mAr/Ag/S fabric in comparison with the unmodified fabric. The temperatures at the peak maximum were comparable with the mAr/Ag fabric (Figure 14). The heat of thermal degradation increased by 20 J/g for both modified meta-aramid fabrics.

The initial temperature of thermal degradation for the unmodified pAr fabric was 525 °C. The process took place in two stages, with the maximum endothermic peaks at 549 °C (first stage) and 581 °C (second stage) (Figure 13b, Table S2). The heat of thermal decomposition was 271 J/g. For the pAr/Ag fabric, at a temperature of 386 °C, thermal decomposition of PVP occurred, with a peak maximum at 430 °C. The heat during the thermal degradation of PVP was 18 J/g.

After the application of AgNWs, the initial temperature during the thermal decomposition of para-aramid fabric increased by 14 °C. The temperature at the peak maximum of the first stage was higher by about 10 °C, and at the peak maximum of second stage, did not change compared to the unmodified fabric. The heat during the thermal decomposition of the pAr/Ag fabric was higher by 49 J/g.

For AgNW- and silane-modified para-aramid fabrics, heating above 290 °C resulted in the thermal degradation of silanes. This occurred at a temperature of 293 °C, with a peak maximum at 321 °C, for the pAr/Ag + S fabric, and at 314 °C, with a peak maximum at 332 °C, for the pAr/Ag/S fabric. The PVP thermal decomposition began at a temperature of 401 °C, with a peak maximum at 430 °C, for the pAr/Ag + S fabric, and at 399 °C, with a peak maximum at 432 °C, for the pAr/Ag/S fabric.

The Ag + S and Ag/S modifications improved the thermal stability of the para-aramid fabric. The application of silanes decreased the initial temperature during thermal degradation in comparison with the fabric coated with only AgNWs, but it was still higher by 6 °C and by 8 °C compared to unmodified fabric after Ag + S and Ag/S coating application. The temperature at the peak maximum of the first thermal degradation stage

increased by 5 °C for the pAr/Ag + S and by 7 °C for the pAr/Ag/S fabric, and for the second stage, these values did not change for either of the modified fabrics (Figure 14). The heat during thermal degradation was higher by 12 J/g and 19 J/g for the pAr/Ag + S and pAr/Ag/S fabrics, respectively.

3.9. Antibacterial Properties

Some occupational conditions of increased humidity and temperature favor the development of microorganisms. Therefore, we also tested the activity of the modified aramid fabrics against representative examples of two major classes of bacteria: Gram-negative (*Klebsiella pneumoniae*) and Gram-positive (*Staphylococcus aureus*).

All modified aramid fabrics exhibited antibacterial properties. The reduction in bacterial growth (R) against *K. pneumoniae* amounted to 99.9% for the mAr/Ag and pAr/Ag fabrics (Table 3). The lower value was observed against *S. aureus* for the mAr/Ag fabric (90.9%), and the lowest for the pAr/Ag fabric (72.0%).

Table 3. Antibacterial properties of modified aramid woven fabrics.

	mAr/Ag		mAr/Ag + S		mAr/Ag/S	
	S. aureus	*K. pneumoniae*	*S. aureus*	*K. pneumoniae*	*S. aureus*	*K. pneumoniae*
Concentration of inoculum, CFU/mL	1.8×10^5	1.5×10^5	1.8×10^5	1.5×10^5	1.8×10^5	1.5×10^5
Reduction in bacterial growth, R	90.9%	99.9%	90.0%	90.0%	90.0%	90.0%
Value of the bacteriostatic coefficient, S *	7.7	7.8	7.7	7.8	8.1	8.3
Value of the bactericidal coefficient, L **	3.1	3.2	3.1	3.2	3.2	3.4
	pAr/Ag		pAr/Ag + S		pAr/Ag/S	
	S. aureus	*K. pneumoniae*	*S. aureus*	*K. pneumoniae*	*S. aureus*	*K. pneumoniae*
Concentration of inoculum, CFU/mL	1.8×10^5	1.5×10^5	1.8×10^5	1.5×10^5	1.8×10^5	1.5×10^5
Reduction in bacterial growth, R	72.0%	99.9%	90.0%	95.7%	90.0%	90.0%
Value of the bacteriostatic coefficient, S *	5.5	7.9	7.7	7.8	8.1	8.3
Value of the bactericidal coefficient, L **	0.6	3.0	3.1	3.2	3.2	3.4

* The bacteriostatic coefficient (S)—the inhibition of bacterial cellular activity without directly causing bacterial death, calculated according to Equation: $S = \lg C_t - \lg T_t$. ** The biocidal coefficient (L)—the reduction in the number of viable colony-forming units in relation to the density of the inoculum at incubation time, calculated according to Equation: $L = \lg C_0 - \lg T_t$, where T_t is the concentration of the bacteria for the coated fabrics after 21 h + 48 h incubation time, and C_0 and C_t are the concentrations of bacteria on the unmodified fabrics, as control samples, after 0 h and 21 h + 48 h, respectively.

For Ag + S- and Ag/S-modified mAr fabric and pAr/Ag/S fabric, the reduction in bacterial growth (R) amounted to 90.0% against both bacteria, and for the pAr/Ag + S fabric, it amounted to 95.7% against *K. pneumoniae* and to 90.0% against *S. aureus*. All modified fabrics demonstrated bacteriostatic and bactericidal properties, because the value of the biostatic coefficient was greater than two and the value of the biocidal coefficient was greater than zero. Ag/S modified aramid fabric had stronger bacteriostatic and bactericidal properties against *K. pneumoniae* than against *S. aureus*.

Amato et al. [31] noticed that colloidal silver exhibits stronger activity against Gram-negative (*E. coli*) than Gram-positive (*S. aureus*). Giesz et al. [6] studied the antibacterial properties of cotton fabric modified by AgNWs. The reduction in bacteria; growth on AgNW-modified cotton fabric for Gram-negative *K. pneumoniae* (97.7%) was also higher than for *S. aureus* (94.7%). The stronger antibacterial properties observed against Gram-

negative (*K. pneumoniae*) bacteria may have been due to differences in the structures of the bacteria cells. Gram-negative bacteria have thin cell walls composed of several layers of peptidoglycan, which is additionally surrounded by an outer cell membrane containing fatty substances and polysaccharides, giving it the characteristic of low permeability. Gram-positive bacteria have thick cell walls made of many peptidoglycans, without an outer cell membrane [32].

4. Conclusions

We investigated the influence of modifications with AgNWs and silanes on the thermal management, thermal stability, and antibacterial properties of meta- and para-aramid woven fabrics. Two modification approaches were developed. The first is the mixture (Ag + S) method, by which silanes were added to AgNWs colloid and applied to the fabric. The second is the layer-by-layer (Ag/S) method, in which a silane layer was applied to the AgNW-modified woven fabric.

Aramid fabrics modified using the Ag + S and Ag/S methods had lower surface temperatures, by about 3 °C for meta- and by about 2 °C for para-aramid fabrics in comparison with the unmodified fabrics. In the temperature range of 35–40 °C, modified fabrics showed better thermal insulation properties and more effective reflection of electromagnetic radiation in the infrared range.

The analysis of DSC and TG/DTG showed that, after modifications with Ag + S and Ag/S, the para-aramid fabric had better thermal stability. The TG/DTG results showed that, after the AgNWs and silane modifications, the initial temperature during the para-aramid thermal degradation process increased from 554 °C to about 560 °C, and the weight loss decreased from 60% to 47%. For the meta-aramid fabric, the initial temperature decreased from 417 °C to about 402 °C, and the weight loss increased from 47% to 49%. The results of the DSC analysis showed that the initial temperature of thermal degradation increased from 525 °C to about 533 °C for the para-aramid fabric and decreased from 411 °C to about 406 °C for the meta-aramid fabric.

The silver nanowire and silane coatings will allow us to provide aramid fabrics with antibacterial properties against *Staphylococcus aureus* and *Klebsiella pneumonia* bacteria that are comparable to fabrics modified with only AgNWs. The antibacterial activity was slightly higher for Gram-negative bacteria.

Ag + S and Ag/S coatings revealed good thermal insulation, thermal stability, and antibacterial properties for both fabrics, with slightly higher thermal stability for the para-aramid fabric.

Aramid fabrics coated with Ag + S and Ag/S have great potential to be used as novel, multifunctional textile materials. Thanks to the combination of the obtained properties, such materials can be used in extreme temperature conditions. They can also provide thermal comfort and protection against the development of microorganisms when used as materials for the production of clothing for high-risk professions, as interior furnishings, for the production of window blinds and curtains, or in biomedical applications.

The developed modified aramid textile materials are intended for repeated use, and in order to protect life and health, they should maintain a set of barrier properties throughout the entire use cycle. Therefore, further research is planned in order to assess the impacts of use and aging of such modified materials on their functional properties. This will allow us to obtain knowledge regarding further treatment of the studied group of materials after their usefulness as protective materials has ended. This will provide us with knowledge essential for their disposal/recycling, which is extremely important for environmental protection.

Supplementary Materials: The following supporting information can be downloaded at: https://www.mdpi.com/article/10.3390/coatings13111852/s1, Table S1: TG/DTG data for meta- and para-aramid woven fabrics, unmodified and modified with AgNWs by the mixture and layer-by-layer methods; Table S2: DSC data for meta- and para-aramid woven fabrics, unmodified and modified with AgNWs by the mixture and layer-by-layer methods.

References

1. Song, G.; Ding, D.; Chitrphiromsri, P. Numerical Simulations of Heat and Moisture Transport in Thermal Protective Clothing under Flash Fire Conditions. *Int. J. Occup. Saf. Ergon.* **2008**, *14*, 89–106. [CrossRef]
2. Fu, M.; Weng, W.; Yuan, H. Thermal Insulations of Multilayer Clothing Systems Measured by a Bench Scale Test in Low Level Heat Exposures. *Int. J. Cloth. Sci. Technol.* **2014**, *26*, 412–423. [CrossRef]
3. Naeem, J.; Mazari, A.; Naeem, M.S.; Rasheed, A.; Ahmad, F.; Ahmad, S. Durability of Metallic Coating for Improvement of Thermal Protective Performance of Firefighter Protective Clothing. *J. Text. Inst.* **2022**, *114*, 820–833. [CrossRef]
4. Sarier, N.; Onder, E. Organic Phase Change Materials and Their Textile Applications: An Overview. *Thermochim. Acta* **2012**, *540*, 7–60. [CrossRef]
5. Balamurugan, M.; Saravanan, S.; Soga, T. Coating of Green-Synthesized Silver Nanoparticles on Cotton Fabric. *J. Coat. Technol. Res.* **2017**, *14*, 735–745. [CrossRef]
6. Giesz, P.; Mackiewicz, E.; Nejman, A.; Celichowski, G.; Cieślak, M. Investigation on Functionalization of Cotton and Viscose Fabrics with AgNWs. *Cellulose* **2017**, *24*, 409–422. [CrossRef]
7. Jones, R.S.; Draheim, R.R.; Roldo, M. Silver Nanowires: Synthesis, Antibacterial Activity and Biomedical Applications. *Appl. Sci.* **2018**, *8*, 673. [CrossRef]
8. Kim, J.-H.; Ma, J.; Jo, S.; Lee, S.; Kim, C.S. Enhancement of Antibacterial Properties of a Silver Nanowire Film via Electron Beam Irradiation. *ACS Appl. Bio Mater.* **2020**, *3*, 2117–2124. [CrossRef]
9. Kiran Kumar, A.B.V.; Wan Bae, C.; Piao, L.; Kim, S.H. Silver Nanowire Based Flexible Electrodes with Improved Properties: High Conductivity, Transparency, Adhesion and Low Haze. *Mater. Res. Bull.* **2013**, *48*, 2944–2949. [CrossRef]
10. Kaikanov, M.; Kemelbay, A.; Amanzhulov, B.; Demeuova, G.; Akhtanova, G.; Bozheyev, F.; Tikhonov, A. Electrical Conductivity Enhancement of Transparent Silver Nanowire Films on Temperature-Sensitive Flexible Substrates Using Intense Pulsed Ion Beam. *Nanotechnology* **2021**, *32*, 145706–145715. [CrossRef]
11. Nejman, A.; Baranowska-Korczyc, A.; Ranoszek-Soliwoda, K.; Jasińska, I.; Celichowski, G.; Cieślak, M. Silver Nanowires and Silanes in Hybrid Functionalization of Aramid Fabrics. *Molecules* **2022**, *27*, 1952. [CrossRef]
12. Tomiyama, T.; Mukai, I.; Yamazaki, H.; Takeda, Y. Optical Properties of Silver Nanowire/Polymer Composite Films: Absorption, Scattering, and Color Difference. *Opt. Mater. Express* **2020**, *10*, 3202–3214. [CrossRef]
13. Luu, Q.N.; Doorn, J.M.; Berry, M.T.; Jiang, C.; Lin, C.; May, P.S. Preparation and Optical Properties of Silver Nanowires and Silver-Nanowire Thin Films. *J. Colloid Interface Sci.* **2011**, *356*, 151–158. [CrossRef]
14. Nateghi, M.R.; Shateri-Khalilabad, M. Silver Nanowire-Functionalized Cotton Fabric. *Carbohydr Polym.* **2015**, *117*, 160–168. [CrossRef]
15. Baranowska-Korczyc, A.; Mackiewicz, E.; Ranoszek-Soliwoda, K.; Nejman, A.; Trasobares, S.; Grobelny, J.; Cieślak, M.; Celichowski, G. A SnO_2 Shell for High Environmental Stability of Ag Nanowires Applied for Thermal Management. *RSC Adv.* **2021**, *11*, 4174–4185. [CrossRef]
16. Hsu, P.C.; Liu, X.; Liu, C.; Xie, X.; Lee, H.R.; Welch, A.J.; Zhao, T.; Cui, Y. Personal Thermal Management by Metallic Nanowire-Coated Textile. *Nano Lett.* **2015**, *15*, 365–371. [CrossRef]
17. *PN-P-04613:1997*; Textiles—Knitted and Stitch Bonded Fabrics—Determination of Mass per Unit Length and Mass per Unit Area. Polish Standardization Committee: Warsaw, Poland, 1997.

18. *PN-EN ISO 5089:1999*; Textiles—Determination of Thickness of Textiles and Textile Products. Polish Standardization Committee: Warsaw, Poland, 1999.
19. *PN-EN ISO 9237:1998*; Textiles—Determination of Permeability of Fabrics to Air. Polish Standardization Committee: Warsaw, Poland, 1998.
20. *AATCC 100-2012*; Assessment of Antibacterial Finishes on Textile Materials. American Association of Textile Chemists & Colorists: Research Triangle Park, NC, USA, 2012.
21. *PN-EN ISO 20743*; Determination of the Antibacterial Activity of Finished Products with Antibacterial Finish. Absorption Method. Polish Standardization Committee: Warsaw, Poland, 2021.
22. Lee, C.Y.; Van Le, Q.; Kim, C.; Kim, S.Y. Use of Silane-Functionalized Graphene Oxide in Organic Photovoltaic Cells and Organic Light-Emitting Diodes. *Phys. Chem. Chem. Phys.* **2015**, *17*, 9369–9374. [CrossRef]
23. Girardi, F.; Bergamonti, L.; Isca, C.; Predieri, G.; Graiff, C.; Lottici, P.P.; Cappelletto, E.; Ataollahi, N.; Di Maggio, R. Chemical–Physical Characterization of Ancient Paper with Functionalized Polyamidoamines (PAAs). *Cellulose* **2017**, *24*, 1057–1068. [CrossRef]
24. Wang, C.B.; Deo, G.; Wachs, I.E. Interaction of Polycrystalline Silver with Oxygen, Water, Carbon Dioxide, Ethylene, and Methanol: In Situ Raman and Catalytic Studies. *J. Phys. Chem. B* **1999**, *103*, 5645–5656. [CrossRef]
25. Jena, K.K.; Alhassan, S.M.; Tiwari, A.; Hihara, L.H. Functional Nano-Coating Materials by Michael Addition and Ring-Opening Polymerization: Reactivity, Molecular Architecture and Refractive Index. *Sci. Rep.* **2018**, *8*, 11912. [CrossRef]
26. Lian, Y.; Yu, H.; Wang, M.; Yang, X.; Li, Z.; Yang, F.; Wang, Y.; Tai, H.; Liao, Y.; Wu, J.; et al. A Multifunctional Wearable E-Textile via Integrated Nanowire-Coated Fabrics. *J. Mater. Chem. C* **2020**, *8*, 8399–8409. [CrossRef]
27. Liu, H.; Lee, Y.Y.; Norsten, T.B.; Chong, K. In Situ Formation of Anti-Bacterial Silver Nanoparticles on Cotton Textiles. *J. Ind. Text.* **2014**, *44*, 198–210. [CrossRef]
28. Usmanova, L.S.; Ziganshin, M.A.; Rakipov, I.T.; Lyadov, N.M.; Klimovitskii, A.E.; Mukhametzyanov, T.A.; Gerasimov, A.V. Microspherical Particles of Solid Dispersion of Polyvinylpyrrolidone K29-32 for Inhalation Administration. *Biomed. Res. Int.* **2018**, *2018*, 2412156. [CrossRef] [PubMed]
29. Zhenhua, S.; Yanfen, Z.; Wenyue, L.; Shaojuan, C.; Shihua, Y.; Jianwei, M. Preparation of Silver-Plated Para-Aramid Fiber by Employing Low-Temperarure Oxygen Plasm Treatment and Dopamine Functionalization. *Coatings* **2019**, *9*, 559.
30. Morsi, M.A.; Abdelrazek, E.M.; Abdelghany, A.M.; Badr, S.I. Morphological, Thermal and Electrical Properties of (PEO/PVP)/Au Nanocomposite Before and After Gamma-Irradiation. *J. Res. Updat. Polym. Sci.* **2017**, *6*, 45–54.
31. Amato, E.; Diaz-Fernandez, Y.A.; Taglietti, A.; Pallavicini, P.; Pasotti, L.; Cucca, L.; Milanese, C.; Grisoli, P.; Dacarro, C.; Fernandez-Hechavarria, J.M.; et al. Synthesis, Characterization and Antibacterial Activity against Gram Positive and Gram Negative Bacteria of Biomimetically Coated Silver Nanoparticles. *Langmuir* **2011**, *27*, 9165–9173. [CrossRef]
32. Cieślak, M.; Kowalczyk, D.; Krzyżowska, M.; Janicka, M.; Witczak, E.; Kamińska, I. Effect of Cu Modified Textile Structures on Antibacterial and Antiviral Protection. *Materials* **2022**, *15*, 6164. [CrossRef]